ARTICLE

Preparation and Characterization of Microporous Layers on Titanium

Shin-ichi Tanaka,*,† Haruki Tobimatsu,‡ Yuuki Maruyama,‡ Toshiyuki Tanaki,§ and Gregory Jerkiewicz*,||

Department of Materials Science and Engineering and Advanced Engineering School, Kurume National College of Technology, 1-1-1 Komorino, Kurume, Fukuoka 830-8555, Japan, Tokyo Metropolitan Industrial Technology Research Institute, 3-7-10 Akebono-cho, Tachikawa, Tokyo 190-0012, Japan, and Department of Chemistry, Queen's University, 90 Bader Lane, Kingston, Ontario K7L 3N6, Canada

ABSTRACT Microporous layers on titanium (Ti) are formed by chemical treatment in highly concentrated alkaline media, and their properties and growth mechanism are examined using electrochemical techniques, in situ resistometry, scanning electron microscopy (SEM), grazing-incident X-ray diffraction (GIXRD), and glow discharge optical emission spectroscopy (GD-OES). Chemical treatment in a 5 M aqueous KOH solution yields results superior to those from the same treatment in a 5 M aqueous NaOH solution, while a 3 M aqueous LiOH solution does not produce porous layers. The cation constituting the solution plays a vital role in the process. An SEM analysis reveals that the KOH solution is the most effective in forming microporosity and that the longer the treatment time, the more porous the near-surface layer. The results of GIXRD analysis show the presence of $Na_2Ti_5O_{11}$ and $K_2Ti_6O_{13}$ in the layers formed in the NaOH and KOH solutions, respectively; in the case of the LiOH solution, TiO_2 is formed. Chemical treatment in the NaOH and KOH solutions resembles a general corrosion process with the existence of local cathodic and anodic sites. The reduction reaction produces H_2, some of which becomes absorbed in the near-surface region of Ti, while the oxidation reaction produces the above-mentioned compounds and/or an oxide layer. The presence of hydrogen (H) within the solid is detected using GD-OES. The H-containing near-surface layer partially dissolves, yielding a microporous structure. The development and dissolution of the H-containing near-surface layer of Ti upon chemical treatment in the NaOH and KOH solutions are confirmed by resistometry measurements. They point to the formation of a compact passive layer on Ti upon exposure to the LiOH solution.

KEYWORDS: electrochemistry • titanium • porous layers • chemical treatment • alkaline solutions

INTRODUCTION

Titanium (Ti) and its alloys are relatively light and inexpensive; they possess unique chemical, physical, and physiological properties, such as good ductility, a high tensile modulus, a high fatigue strength, and an elasticity modulus that matches that of the human bone. In addition, they resist corrosion in body fluids and are compatible with the human body. All of these characteristics make Ti and its alloys excellent biomaterials that are applied in the manufacture of artificial bones and dental and orthopedic implants. The applicability of Ti and its alloys as biomaterials is linked to the surface pretreatment that needs to be applied to enhance the adhesion of the body tissue to the implant material (1−12). Hydroxyapatite coatings are often used for Ti orthopedic and dental implants. They are formed by plasma spraying under high-temperature conditions (4, 5), although this approach induces changes in the crystal structure of the substrate, reduces biocorrosion resistance, and develops cracks. Other coating methods, such as laser deposition (6), sol−gel dipping (7, 8), or electrophoresis (9, 10), are also employed as suitable treatments.

The most common treatment procedure involves surface activation of Ti through immersion in a concentrated aqueous solution of NaOH for about 24 h and at a temperature (T) of 353 K (1−3). This results in the formation of a porous structure (up to 1 μm in thickness) that is very effective at providing nucleation points for calcium phosphate precipitation and integration within the surface layer of the Ti implant.

We investigated the mechanism of formation of a porous layer on Ti in an aqueous NaOH solution (11, 13, 14). Our results indicate that the existence of absorbed hydrogen (H_{abs}) in the near-surface region of Ti is a very important factor that influences the preparation of the porous layers. The chemical treatment resembles a general corrosion process that involves the existence of local cathodic and anodic regions. In a cathodic region, the hydrogen evolution reaction (HER) takes place, and it involves H_{ads} as a reaction intermediate. H_{ads} can undergo absorption to form H_{abs}, which then diffuses into the bulk of the metal host (the process is driven by a concentration gradient that gives rise to a gradient of the Gibbs energy for H_{abs}). The Ti surface layer containing H_{abs} dissolves more readily in concentrated alkaline solutions than untreated Ti (11), and its dissolution

* E-mail: s-tanaka@kurume-nct.ac.jp (S.-i.T.), gregory.jerkiewicz@chem.queensu.ca (G.J.).

Received for review July 15, 2009 and accepted September 17, 2009

† Department of Materials Science and Engineering, Kurume National College of Technology.

‡ Advanced Engineering School, Kurume National College of Technology.

§ Tokyo Metropolitan Industrial Technology Research Institute.

|| Queen's University.

DOI: 10.1021/am900474h

Published on Web 09/29/2009

creates a porous layer. Therefore, hydrogen absorption into Ti is an important factor that needs to be taken into account when analyzing the mechanism of formation of porous structures on Ti and Ti-containing alloys. However, the detection of H_{abs} in a narrow surface range and the quantification of the process are difficult and require the application of suitable materials science techniques.

Resistometry is a convenient technique for in situ monitoring of the corrosion of steels (15, 16) and for the formation of passive films on iron (17, 18). It can be applied to monitor passivation and corrosion processes on other metals. Resistometry relates the change in the electrical resistance (R) to either a decrease of the material's dimensions (due to metal dissolution through corrosion) or a modification of its electrical resistivity (ρ) caused by compositional changes, such as hydrogen absorption (19−22).

In this paper, we report on the preparation of microporous layers on Ti by chemical treatment in highly concentrated alkaline media that contain different alkali cations. Their three-dimensional structure, surface morphology, and chemical composition are characterized using several materials science techniques. Electrochemical techniques are employed to elucidate the mechanism of their development. The role of H_{abs} in the near-surface region of Ti is discussed in terms of the mechanism of formation of the microporous layers.

EXPERIMENTAL SECTION

Ti Sample Preparation. Ti electrodes in the form of wires and sheets were employed. Ti wires were used in resistometry measurements, and Ti sheets were used in all other experiments. The Ti wires (Nilaco Co., 99.6%, 0.10 mm in diameter and 100 mm in length) were connected to a copper (Cu) wire and covered with a shrinkable Teflon. Each specimen was degreased in acetone under reflux, dried, and eventually rinsed with distilled and deionized water (Millipore Milli-Q). Ti sheets (Nilaco Co., 99.5%, 1.0 mm in thickness) were used for electrochemical, scanning electron microscopy (SEM), grazing-incident X-ray diffraction (GIXRD), and glow discharge optical emission spectroscopy (GD-OES) measurements. They were degreased and annealed in a vacuum (pressure $\leq 1.3 \times 10^{-8}$ bar) to homogeneity at $T = 1073$ K for 4 h. High vacuum is required to eliminate the thermal formation of oxides, nitrides, carbides, or other compounds. Following the annealing, the specimens were polished using polishing paper, diamond abrasive (1 μm), and colloidal silica (0.04 μm) until a mirror-like finish of roughness below 0.04 μm was obtained. Then, they were degreased with acetone in an ultrasonic bath. Each specimen was connected to a Cu wire using a silver acrylic acid resin (Fujikura Kasei Co., D-550) and covered with an epoxy resin (Huntsman Advanced Materials Co., Araldite Rapid type). Finally, each sample was etched in an aqueous etching solution containing hydrofluoric acid (HF, 2% by volume) and nitric acid (HNO_3, 4% by volume) at room temperature for several seconds and then rinsed with distilled and deionized water. The geometric surface area of the Ti electrodes was determined using their dimensions. In the case of the finely polished samples, the geometric and real surface areas are equal.

Chemical Treatment of Ti. Ti wires were treated by immersion in (i) a 5 M aqueous NaOH solution; (ii) a 5 M aqueous KOH solution, or (iii) a 3 M aqueous LiOH solution. In the case of the LiOH solution, the concentration was only 3 M because the solubility of LiOH in water is lower (12.3 g per 100 g of water at $T = 293$ K) than that of NaOH or KOH (23). All alkaline solutions were prepared using analytical-grade chemicals (Kanto Chemical Co.) and distilled and deionized water (Millipore Milli-Q water). Chemical treatment was carried out at $T = 353$ K in a Teflon vessel to reduce any contamination due to glass dissolution.

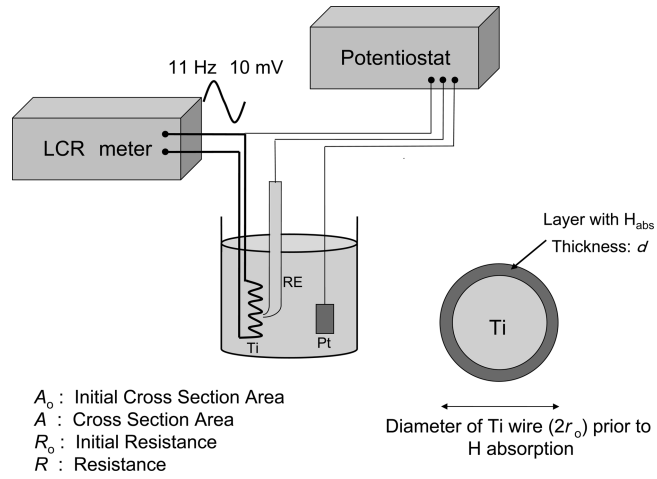

FIGURE 1. Conceptual diagram of the resistometry experimental setup.

Materials Characterization. Materials characterization of Ti sheet specimens was performed at various stages of research. Following electrochemical measurements, the specimens were rinsed with distilled and deionized water for ca. 30 s and carefully dried using a stream of dry N_2(g) for ca. 30 s. The surface morphology was examined using SEM (Hitachi Co., model S-2380N) and the crystallographic structure using GIXRD (JEOL Co., model JDX-3530). The incident angle (θ) of the X-ray beam was set at 1°, and the specimen was rotated during the measurement. A hydrogen depth profile was acquired using GD-OES (Horiba Co., model JY-5000RF) combined with argon (Ar)-ion sputtering. The emission spectrum is characteristic of the atomic number and, therefore, allows for a fast and simultaneous identification of the elements constituting the sample. GD-OES provides information about both the bulk and surface chemical composition with high sensitivity and minimal analysis time and can detect hydrogen that is impossible to identity using other surface science techniques, such as X-ray photoelectron spectroscopy or Auger electron spectroscopy.

Electrochemical Measurements. Electrochemical measurements were done using a potentiostat (Hokuto Denko Co., model HA-501), a function generator (Hokuto Denko Co., model HB-104), and a digital multimeter (Sanwa Electric Instrument Co., model PC-20). Cathodic and anodic potentiodynamic polarization curves were acquired at a scan sweep rate (s) of 0.1 V min^{-1}. During acquisition of the polarization curves, the alkaline electrolytes were deaerated by bubbling Ar gas through the cell. The potential of the working electrode was monitored against a silver/silver chloride reference electrode placed in a saturated solution of KCl [Ag/AgCl/KCl(sat)]; it was converted to the reversible hydrogen electrode potential scale. The working, counter, and reference electrodes were in separate compartments of a Teflon cell.

Resistometry Measurements. Figure 1 shows the setup used in resistometry measurements. The electrical resistance (R) of Ti wires during the formation of a porous layer was measured using an alternating current (ac) technique in which an *LCR* meter (where L refers to the inductance, C to the capacitance, and R to the resistance; Hioki E. E. Co., model LCR Hi-Tester 3522-50) was used to apply an ac signal with a 10 mV peak-to-peak voltage at a frequency of 11 Hz. We used a low frequency of the ac signal to minimize current leakage to the surroundings. The electrical resistance is displayed as a relative resistance

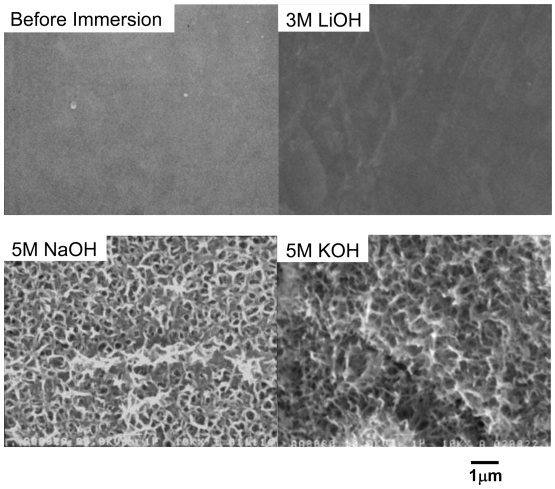

FIGURE 2. SEM micrographs for untreated Ti and three Ti specimens after their immersion in 3 M LiOH, 5 M NaOH, and 5 M KOH aqueous solutions for $t = 24$ h at $T = 353$ K.

change (RR_0^{-1}) as a function of time (t), where R_0 is the initial resistance (at $t = 0$) and refers to a specimen free of any absorbed hydrogen or hydride.

RESULTS AND DISCUSSION

SEM Characterization. Figure 2 shows SEM micrographs of four Ti specimens, one prior to the treatment and three after their immersion in the three different alkaline solutions for $t = 24$ h at $T = 353$ K. The morphology of the porous layers strongly depends on the nature of the alkali cation present in the solution; a porous layer is formed only upon Ti exposure to 5 M aqueous KOH or 5 M aqueous NaOH solutions. Elsewhere (1−3), it was reported that a porous layer on Ti can be obtained in a concentrated NaOH solution, but our SEM data demonstrate that the application of concentrated KOH yields comparable results. Kokubo and Takamada (24) analyzed the biocompatibility of porous Ti layers and reported that the porous layer on Ti prepared in aqueous KOH facilitates the precipitation of hydroxyapatite in a simulated body fluid saturated with calcium phosphate. This is an important observation that justifies the purpose and importance of the treatment of Ti in strong alkaline media. On the other hand, a porous layer is not formed in the case of Ti immersion in 3 M aqueous LiOH, and the surface morphology of the specimen only slightly changed as compared to the same sample before chemical treatment. Thus, we conclude that the preparation of porous layers on Ti strongly depends on the nature of the cation constituting the alkaline solution (see the section below).

We performed research to compare the effectiveness of KOH versus that of NaOH. In a separate series of experiments, we exposed freshly prepared Ti samples to 5 M aqueous solutions of KOH and NaOH for 1, 6, 12, and 24 h and at $T = 353$ K. In Figure 3, we show SEM micrographs for the Ti samples exposed for 1, 6, and 12 h, while the micrographs presented in Figure 2 show analogous results for 24 h. They reveal a porous (fibrous) structure that becomes more pronounced as the exposure time increases. However, in the case of the KOH solution, a porous structure is observed already after exposure for 1 h, while in the case of NaOH, there is hardly any porous structure and a longer exposure time is required to achieve the same effect. The results reveal that the morphology of the samples depends on the nature of the solution and, more specifically, on the nature of the cation. In the case of KOH, the pores are well-defined and large, while in the case of NaOH, they are small. These results demonstrate that the 5 M aqueous solution of KOH is more suitable for the formation of porous layers on Ti than the NaOH one.

GIXRD Analysis. Figure 4 shows four GIXRD patterns: three for Ti exposed to the three alkaline solutions and one for untreated Ti; the latter serves as a reference. The GIXRD patterns reveal sharp peaks that are characteristic of Ti and broad peaks that are related to the presence of porous layers; these broad peaks are not observed in the case of Ti immersion in the 3 M aqueous LiOH solution. The broad nature of the peaks is indicative of a relatively small thickness of the porous layers. The GIXRD analysis (value of 2θ) allows us to identify $Na_2Ti_5O_{11}$ as a compound present within the porous layer that is formed upon Ti immersion in the NaOH solution. We do not detect any sodium titanate hydrogel (25), and our results are in agreement with previously reported data as well as validate our interpretation (26, 27). The GIXRD analysis also allows us to identify potassium titanate ($K_2Ti_6O_{13}$) as a compound present within the porous layer that is formed upon Ti immersion in the KOH solution. The peaks corresponding to the titanate are very weak and not clearly defined. Elsewhere, Kim et al. reported that the porous film obtained in the NaOH solution consists mainly of an amorphous sodium titanate hydrogel (26). Although the porous layers certainly contain alkali titanates (except for the case of Ti immersion in the LiOH solution), they can also include water, which is known to broaden the diffraction peaks and to lower their intensities (25−27). However, the peak broadening can also originate from a change in the average crystallite size, the introduction of lattice defects, and/or an increase in the internal strain. At the present time, we are unable to determine which of the three above-mentioned phenomena is responsible for the peak broadening that we observe.

In the case of Ti treatment in the 3 M aqueous LiOH solution, the GIXRD results did not reveal any peaks characteristic of an alkali titanate but show a small peak characteristic of a thin surface oxide. Metallic Ti is very reactive, and the thin oxide layer develops upon exposure of the metal to the LiOH solution. These results corroborate our interpretation of SEM data, which demonstrate that porous layers on Ti cannot develop in an aqueous LiOH solution. We investigated the influence of the NaOH solution concentration on the formation of porous layers and found that they did not develop on Ti when the concentration was 3 M or less (14). Below this critical concentration, the open-circuit potential of Ti was observed to shift toward higher values with increasing immersion time. These results imply that an oxide film is produced spontaneously in a less concentrated

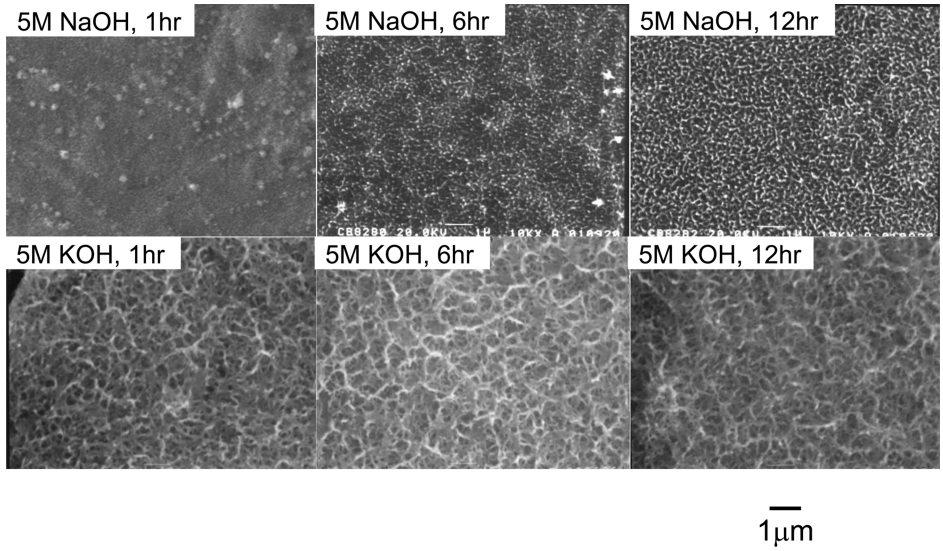

FIGURE 3. SEM micrographs for Ti specimens after their immersion in 5 M NaOH and 5 M KOH aqueous solutions at $T = 353$ K for various exposure times, from 1 to 12 h.

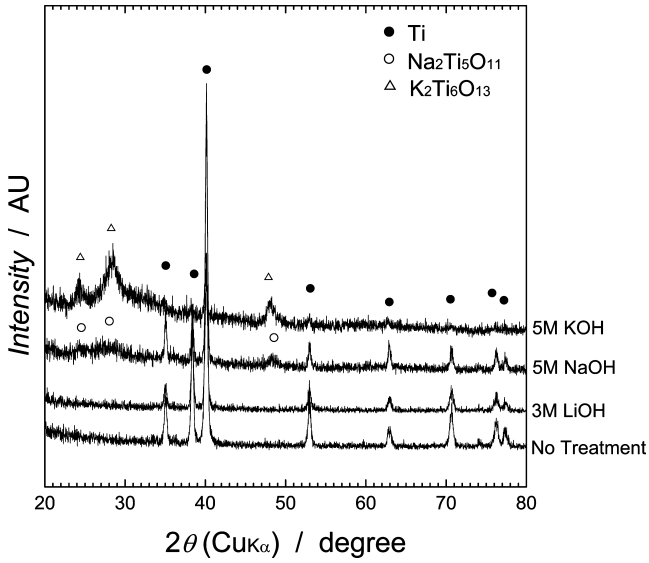

FIGURE 4. GIXRD diffraction patterns for untreated Ti and three Ti specimens following their chemical treatment in 3 M LiOH, 5 M NaOH, and 5 M KOH aqueous solutions for $t = 24$ h at $T = 353$ K. The incident X-ray angle is $\theta = 1°$.

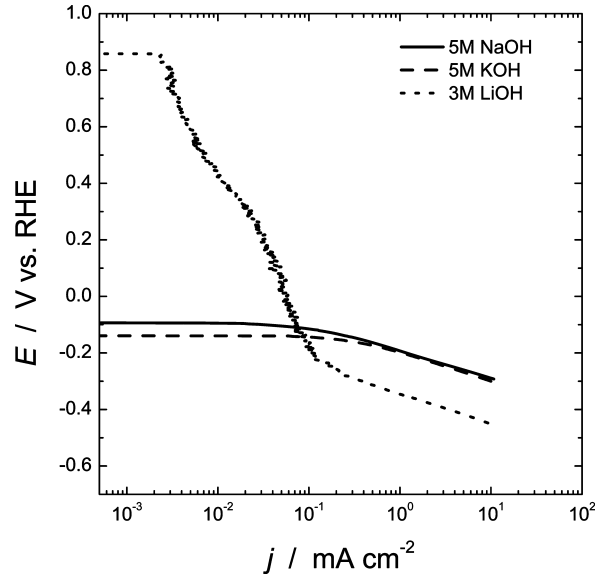

FIGURE 5. Tafel cathodic polarization curves for Ti obtained in 3 M LiOH, 5 M NaOH, and 5 M KOH aqueous solutions; scan rate $s = 0.1$ V min^{-1} and $T = 353$ K.

NaOH solution and that the dissolution of Ti does not take place. Consequently, a porous layer cannot develop.

Electrochemical Characterization. Figure 5 shows polarization curves for freshly prepared Ti electrodes in 5 M aqueous NaOH and KOH solutions and in a 3 M aqueous LiOH solution. They were recorded to assess whether hydrogen generation takes place on Ti and whether some hydrogen becomes absorbed. At this stage of the discussion, it is important to elaborate on an important difference between a typical experimental setup used to study the kinetics and mechanism of HER and our setup. Dedicated kinetic and mechanistic research on HER requires that the electrolyte be free of any gas or soluble species that can undergo a concurrent redox process. Therefore, electrolytes used in dedicated research on HER are carefully deoxygenated by bubbling an inert gas (typically N_2 or Ar); in the presence of dissolved O_2, hydrogen generation and oxygen reduction occur simultaneously. However, we are interested in the hydrogen generation occurring at a Ti electrode that is immersed in a strongly alkaline solution that is exposed to air; thus, the electrolyte contains a certain amount of oxygen (its solubility depends on the electrolyte composition, concentration, and temperature). The polarization curves display a typical Tafel relationship with two linear regions. The curves for Ti in the 5 M aqueous NaOH and KOH solutions have a similar shape that is characteristic of HER, although there is a small contribution to the overall current density from the oxygen reduction reaction (ORR). Because the solutions are not stirred, the concurrently occurring HER and ORR are under diffusion control. However, the behavior of Ti in the 3 M aqueous LiOH solution is different. At lower potentials, there is a clearly defined linear region characteristic of HER (with a small contribution from ORR), but at any given overpotential of HER, the current

density is about 1 order of magnitude smaller than that in the case of NaOH or KOH. This observation is vital in order to explain why porous layers on Ti cannot develop in the 3 M aqueous LiOH solution (see below).

The overpotential deposited hydrogen (H_{OPD}) that resides on the electrode surface is generated in the first step of HER as an intermediate (reaction 1) (28−31). In the case of an electrolytic cell, an external source provides an electron required for this process; in the case of a galvanic cell (a corrosion process is a galvanic-type electrochemical reaction), a concurrently occurring oxidation reaction at a neighboring site is the electron source. The adsorbed H_{OPD} has a certain residence time and can either become involved in the generation of H_2 through one of the two possible pathways depicted in reactions 2 and 2′ or undergo interfacial transfer to become subsurface hydrogen (H_{ss}), reaction 3. The subsurface hydrogen undergoes further transfer into the bulk of the host metal and becomes H_{abs} (reaction 4). Depending on the amount of H_{abs}, either a solid-state hydrogen solution (α phase) develops or a hydride precipitates (large amounts of H_{abs} give rise to the precipitation of titanium hydride in the form of needles).

$$H_2O + e^- \rightarrow H_{OPD} + OH^- \quad (1)$$

$$H_{OPD} + H_2O + e^- \rightarrow H_2\uparrow + OH^- \quad (2)$$

$$H_{OPD} + H_{OPD} \rightarrow H_2\uparrow \quad (2')$$

$$H_{OPD} \rightarrow H_{ss} \quad (3)$$

$$H_{ss} \rightarrow H_{abs} \quad (4)$$

The small current density for HER in the 3 M aqueous LiOH solution indicates that much less H_{OPD} is generated on Ti; thus, there is a significantly smaller flux of hydrogen diffusing into the metal bulk. Consequently, the near-surface region of Ti does not have enough H_{abs} to facilitate the formation of a solid-phase hydrogen solution (metal hydride). Because the latter is vital to make the Ti host dissolve and form a porous structure (11−13), it is apparent that the absence of H_{abs} stabilizes Ti in the 3 M aqueous LiOH solution. The small current density in the −0.25 to +0.85 V potential range is characteristic of a passive layer formation (with a small contribution from ORR).

The polarization curves can be used to determine the exchange current density (j_0) for the HER, assuming that the contribution from ORR is negligible (the experimental work is done at $T = 353$ K, and the solubility of the gases decreases with increasing temperature). The values of j_0 for the HER in 5 M aqueous NaOH and KOH solutions are 9×10^{-5} and 27×10^{-5} A cm^{-2}, respectively. It is interesting to observe that the value of j_0 in the KOH solution is 3 times greater than that in the NaOH one. It is an important observation because it implies that the rate of production of H_{OPD} and the flux of hydrogen that can become absorbed to form a solid-state hydrogen solution (metal hydride) is greater in KOH than in NaOH. This implies that the 5 M aqueous KOH solution facilitates the formation of porous layers on Ti.

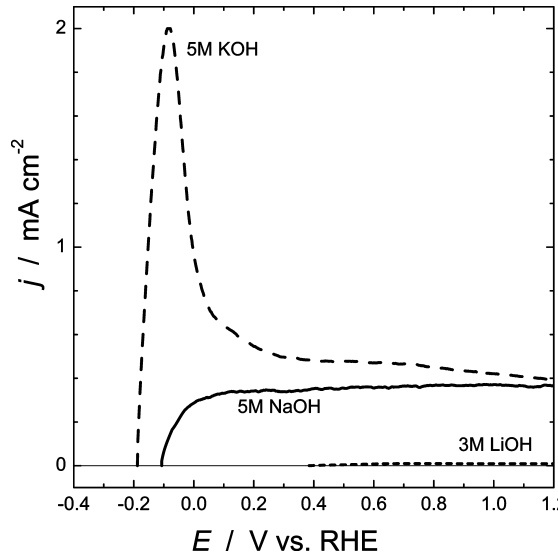

FIGURE 6. Anodic polarization curves of Ti obtained in 3 M LiOH, 5 M NaOH, and 5 M KOH aqueous solutions; scan rate $s = 0.1$ V min^{-1} and $T = 353$ K. The curves were recorded after the Ti specimens immersion in the respective electrolytes for $t = 15$ min at $T = 353$ K.

The anodic behavior of Ti in the three solutions was analyzed by recording polarization curves at $T = 353$ K for 15 min (Figure 6). In the case of the KOH solution, there is a well-defined anodic dissolution peak. In the case of the LiOH solution, the anodic passivation current density is small and there is no dissolution peak. The behavior of Ti in the NaOH solution is qualitatively similar to that in the LiOH one, although the passivation current density is greater. The existence of a well-defined dissolution peak in the KOH solution corroborates our previous conclusions that this electrolyte is very suitable to form porous layers on Ti. In addition, the conclusions deduced on the basis of electrochemical measurements are in good agreement with those obtained from the analysis of SEM micrographs (Figure 2).

Resistometry Measurements. Figure 7 shows RR_0^{-1} vs t plots for Ti in the three alkaline solutions measured at $T = 353$ K. In the case of LiOH, the value of RR_0^{-1} slightly increases ($R > R_0$) and stabilizes after ca. 2 h. The RR_0^{-1} vs t relations for Ti in NaOH and KOH demonstrate a gradual increase of RR_0^{-1} as a function of the time without reaching any limiting value. In the case of Ti immersed in alkaline solutions, there are two surface species that can change the resistance of Ti: a surface passive layer (Ti oxide and alkali titanate) and a surface layer containing H (in either of the two forms mentioned above). The growth of a surface layer containing H progresses until the entire sample is consumed or until it is removed from the highly alkaline environment. On the other hand, a passive layer on Ti (titanium oxide and alkali titanate) tends to grow to a limiting thickness, and the process eventually ceases because the passive layer tends

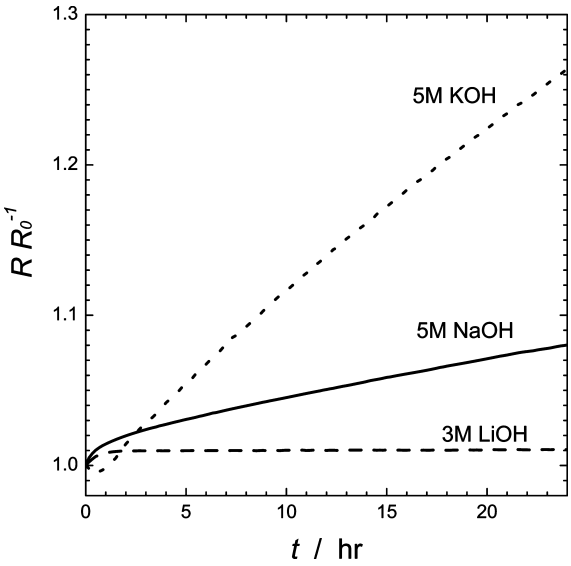

FIGURE 7. Time variation of the relative resistance (RR_0^{-1}) of Ti-wire-shaped specimens during immersion in 3 M LiOH, 5 M NaOH, and 5 M KOH aqueous solutions at $T = 353$ K.

to be compact and imposes a significant barrier to the cationic and anionic species that migrate through it (32−34). The resistometry results for Ti in LiOH point to the growth of a passive layer that reaches a limiting thickness. On the other hand, the resistometry results for Ti in NaOH and KOH solutions are indicative of the progressing development and simultaneous dissolution of a layer containing H. These results support our conclusions drawn from the analysis of electrochemical measurements (32, 33).

The behaviors in NaOH and KOH are qualitatively similar, but for a given time, the value of RR_0^{-1} is significantly higher for KOH than for NaOH. This trend is consistent with our analysis of the SEM micrographs, which demonstrates that the porous layer on Ti grows to a greater extent in KOH than in NaOH. In addition, the electrochemical measurements show that the rate of HER, which produces an H_{ads} spe cies (H_{OPD}), is greater by a factor of ca. 3 in KOH than in NaOH. Because a greater amount of adsorbed H_{OPD} translates into a greater flux of H_{abs} (28, 31), it is apparent that the surface layer of Ti is richer in H_{abs} in the case of KOH than in the case of NaOH.

We elaborate on the decrease of the value of RR_0^{-1} within the first 1 h of immersion in KOH. This is an unusual but reproducible behavior that was also observed by Azumi et al. (35). We propose the following explanation. Prior to its immersion, the Ti specimen is covered with a very thin oxide layer (TiO_2) that develops during the sample preparation, because etched Ti readily oxidizes upon contact with air (oxide-free Ti can only be prepared under high vacuum or neutral gas conditions). Upon its immersion in KOH, a significant flux of H_{abs} facilitates the partial reduction of the passive layer (TiO_2) to a lower state Ti species (Ti^{2+} or Ti^{3+}) that is more conducting than the semiconducting TiO_2 (36). Consequently, the resistivity of the surface layer decreases, giving rise to a lower value of RR_0^{-1}. However, the growth and dissolution of a surface layer containing H_{abs} eventually dominates (for times greater than ca. 1.2 h) the entire surface region and leads to an increase of the value of RR_0^{-1}.

GD-OES Measurements. Figure 8 shows GD-OES depth profiles for three Ti samples after their immersion in the 3 M LiOH, 5 M NaOH, and 5 M KOH solutions at $T = 353$ K and for 24 h. Because the GD-OES experiments are designed to differentiate between oxygen (O) and hydrogen (H) species in the surface and near-surface regions of Ti, we focus our analysis on these elements. The depth profiles show that the sputter time required to remove O and H from the substrate is the longest in the case of the treatment in KOH and the shortest in the case of the treatment in LiOH. Ideally, one would like the sputter time to be converted to depth values. However, this cannot be accomplished for porous samples and for samples whose composition continuously changes because we do not know the sputter yield or the density of the compound that we sputter. The intensity of the H signal as a function of time is complex but in all cases reveals the following features: (i) a steep decrease to a local minimum at t_{min} ($t_{min} = 1$ s for LiOH, 10 s for NaOH, and 45 s for KOH); (ii) a gradual increase to a local maximum at t_{max} ($t_{max} = 2$ s for LiOH, 12 s for NaOH, and 53 s for KOH); (iii) a monotonous decrease with time to a limiting value of zero. The intensity of the O signal as a function of time reveals different features in all three cases: (i) in the case of LiOH, it gradually decreases to zero within ca. 5 s; (ii) in the case of NaOH, it gradually decreases to zero within ca. 18 s, but there are small variations in the signal's intensity within the initial 6 s; (iii) in the case of KOH, it gradually decreases, then rises, reaching a local maximum at ca. 47 s, and then decreases, reaching zero at ca. 70 s. The features observed in the GD-OES depth profiles point to complex Ti/H and Ti/O ratios. The maxima in the H and O signals do not coincide; thus, one may conclude that they are not due to residual water but to O- and H-containing compounds. Although our GIXRD experiments identify $Na_2Ti_5O_{11}$ and $K_2Ti_6O_{13}$ as compounds present within the porous layer on Ti, this technique does not allow us to analyze any variation in the chemical composition as a function of depth. Thus, the results of GD-OES and GIXRD analyses should be treated as complementary. The most important conclusion that can be drawn on the basis of the GD-OES experiments is that the porous layer formed in the 5 M aqueous KOH solution is the thickest because the longest sputter time is required to remove it.

Hydrogen Transfer through Oxide Layers. Ti easily oxidizes upon exposure to air or moisture, yielding TiO_2; the enthalpy of formation of TiO_2(s) is one of the most negative among various transition metals, being $\Delta_f H°(TiO_2) = -944.7$ kJ mol^{-1} (23). Some researchers have suggested that a TiO_2 layer on Ti acts as a barrier to hydrogen absorption (37, 38). However, Ohtsuka et al. reported that, under the conditions of electrolytic hydrogen generation, H atoms can become incorporated in the titanium oxide, transforming it into a hydroxide, and can also reach the underlying Ti substrate, eventually forming a solid-state hydrogen solution (metal hydride) (39). In addition, Azumi

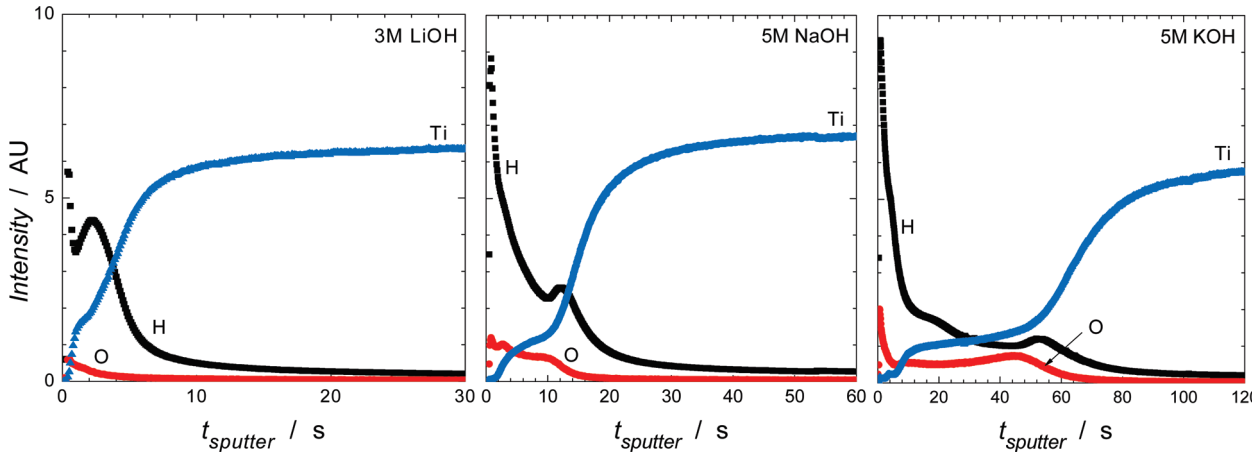

FIGURE 8. GD-OES depth profiles for three Ti specimens after their immersion in 3 M LiOH, 5 M NaOH, and 5 M KOH aqueous solutions for $t = 24$ h at $T = 353$ K.

et al. studied the absorption of hydrogen into Ti in an aqueous H_2SO_4 solution using resistometry and indicated that an anodic oxide layer did not block hydrogen absorption when the Ti was cathodically polarized in the potential region corresponding to HER (22). Although in this study we employed alkaline solutions and did not apply any negative potential, we still obtained results that point to hydrogen absorption into Ti. In our case, the intermediate H_{ads} species that eventually becomes absorbed is generated in a cathodic step of a local (corrosion) galvanic cell. Therefore, our results and data analysis support the notion that a TiO_2 layer on Ti does not create a barrier capable of the complete blocking of hydrogen absorption.

Role of the Cation in the Porosity Development. Our results demonstrate that the morphology and composition of the layers formed on Ti depend on the cation's nature. On the basis of our results and their interpretation, we propose a preliminary explanation of the cation role. The ionic radii of Li^+, Na^+, and K^+ are 0.78, 0.98, and 1.33 Å, respectively (23, 40). Because the three cations possess the same charge but different radii, the electric field around the cation is the strongest in the case of Li^+ and the weakest in the case of K^+. The strength of the ion's electric field translates into a different hydration number (number of water molecules associated with the ion in the solution), which is in the 4−6 range in the case of Li^+, ca. 4 in the case of Na^+, and only 2−4 in the case of K^+ (41). We can relate the strength of the electric field created by a given cation and its hydration number to its ability to form a porous titanate layer. In the case of Li^+, the alkaline treatment develops a compact TiO_2 surface layer and a solid-state hydrogen solution (metal hydride), while in the case of Na^+ and K^+, the treatment develops a porous titanate layer ($Na_2Ti_5O_{11}$ and $K_2Ti_6O_{13}$, respectively) and a solid-state hydrogen solution (metal hydride). The strong electric field associated with Li^+ and its large hydration number prevent it from being incorporated in a crystallographic network comprising Ti^{4+} and O^{2-} ions because a higher energy input is required to dismantle a hydration shell in the case of Li^+ than in the case of Na^+ or K^+. The analysis of the ionic radii and the hydration numbers allows us to conclude that the alkali cation with the largest radius and the smallest hydration number is the most suitable to form porous layers on Ti.

Another important issue related to the formation and stability of the porous layers is the solubility of $Na_2Ti_5O_{11}$ and $K_2Ti_6O_{13}$. To the best of our knowledge, there are no solubility data for these compounds or for the solid-state hydrogen solutions (metal hydrides) in strong alkaline solutions. However, we observe that, in the case of vigorous stirring of the 5 M KOH solution, a thick and well-structured passive layer does not develop. This observation allows us to conclude that the formation of the porous layers occurs through the precipitation of respective alkali cations and titanate anions. The titanate is originally formed through the dissolution of the solid-state hydrogen solution (metal hydride) that is facilitated by the strong alkaline medium. In the absence of stirring or enhanced convection, the immediate vicinity of the solid Ti is saturated with titanate anions and alkali cations, and the precipitation rate is greater than the dissolution one, and consequently a solid titanate deposit develops.

CONCLUSIONS

In summary, we developed a new method of forming microporous layers on Ti that involves chemical treatment in highly concentrated (5 M) aqueous solutions of KOH or NaOH. Similar results cannot be obtained in a highly concentrated (3 M) aqueous solution of LiOH. The microporous layer formed in the KOH solution develops faster, is thicker, and has properties superior to those of the analogous layer prepared in the NaOH solution. The nature of the cation constituting the alkaline solution influences the microporosity development. The smaller the cation and the stronger the electric field that it creates, the lower its capacity for the microporosity development. GIXRD measurements show that the strong alkaline treatment in the NaOH and KOH solutions results in the formation of the respective titanates ($Na_2Ti_5O_{11}$ and $K_2Ti_6O_{13}$). On the other hand, the treatment in the LiOH solution leads to the formation of a compact passive layer made mainly of TiO_2. The growth of the microporous layers on Ti resembles a general corrosion

process that involves local cathodic and anodic sites. The local cathodic reaction generates H_2, some of which becomes absorbed, while the local anodic reaction oxidizes Ti to Ti^{4+} and forms either a titanate or an oxide. GD-OES measurements show the presence of H_{abs} in the near-surface region of the Ti substrate. H_{abs} is a key element in the microporosity development because the H-rich region readily dissolves in strongly alkaline solutions. The treatment in the NaOH and KOH solutions results in a gradual decrease of the resistivity of Ti; this behavior is assigned to the absorption of H and dissolution of the H-containing layer. In the case of the LiOH solution, the resistivity increases to a limiting value that is characteristic of a compact passive layer on Ti (TiO_2).

Acknowledgment. We thank the Kurume National College of Technology for providing financial support to carry out this project. We gratefully acknowledge financial support from the Natural Sciences and Engineering Research Council of Canada through the Discovery Grant and Research Tools and Instruments Grants.

REFERENCES AND NOTES

(1) Kim, H.-M.; Miyaji, F.; Kokubo, T.; Nakamura, T. *J. Ceram. Soc. Jpn.* **1997**, *105*, 111.
(2) Kim, H.-M.; Miyaji, F.; Kokubo, T.; Nishiguchi, S.; Nakamura, T. *J. Biomed. Mater. Res.* **1999**, *45*, 100.
(3) Kim, H.-M.; Miyaji, F.; Kokubo, T.; Nakamura, T. *J. Mater. Sci.: Mater. Med.* **1997**, *8*, 341.
(4) Ducheyne, P.; Van Raemdonck, W.; Heughebaert, J. C.; Heughebaert, M. *Biomaterials* **1986**, *7*, 97.
(5) Thomas, K. A.; Kay, J. F.; Cook, S. D.; Jarcho, M. *J. Biomed. Mater. Res.* **1987**, *21*, 1395.
(6) Bagratashvili, V. N.; Antonov, E. N.; Sobol, E. N.; Popov, V. K.; Howdle, S. M. *Appl. Phys. Lett.* **1995**, *66*, 2451.
(7) Lee, J.; Aoki, H. *Bio-Med. Mater. Eng.* **1995**, *5*, 49.
(8) Li, P.; Groot, K.; Kokubo, T. *J. Sol−Gel Sci. Technol.* **1996**, *7*, 27.
(9) Ducheyne, P.; Radin, S.; Heughebaert, M.; Heughebaert, J. C. *Biomaterials* **1990**, *11*, 244.
(10) Gottlander, M.; Johansson, C. B.; Wennerberg, A.; Albrektsson, T.; Radin, S.; Ducheyne, P. *Biomaterials* **1997**, *18*, 551.
(11) Tanaka, S.; Aonuma, M.; Hirose, N.; Tanaki, T. *J. Electrochem. Soc.* **2002**, *149*, D167.
(12) Matsubara, T.; Oishi, T.; Katagiri, A. *J. Electrochem. Soc.* **2002**, *149*, C89.
(13) Tanaka, S.; Iwatani, T.; Hirose, N.; Tanaki, T. *J. Electrochem. Soc.* **2002**, *149*, F186.
(14) Tanaka, S.; Hirose, N.; Tanaki, T. *J. Electrochem. Soc.* **2005**, *152*, C789.
(15) Denzine, A. F.; Reading, M. S. *Mater. Perform.* **1988**, *37*, 35.
(16) Cella, P. A.; Taylor, S. R. *Corrosion* **2000**, *56*, 951.
(17) Haruyama, S.; Tsuru, T. *Corros. Sci.* **1973**, *13*, 275.
(18) Tsuru, T.; Haruyama, S. *Corros. Sci.* **1976**, *16*, 623.
(19) Gesi, K.; Takagi, Y. *J. Phys. Soc. Jpn.* **1963**, *18*, 306.
(20) Paton, N. E.; Hickman, B. S.; Leslie, D. H. *Metall. Trans.* **1971**, *2*, 2793.
(21) Ariyaratnam, S. V.; Suplise, N. A.; Adem, E. H. *J. Mater. Sci. Lett.* **1987**, *6*, 1349.
(22) Azumi, K.; Asada, Y.; Ueno, T.; Seo, M.; Mizuno, T. *J. Electrochem. Soc.* **2002**, *149*, B422.
(23) Lide, D. R. *CRC Handbook of Chemistry and Physics*, 74th ed.; CRC Press: Boca Raton, FL, 1993.
(24) Kokubo, T.; Takadama, H. *Biomaterials* **2006**, *27*, 2907.
(25) Kokubo, T. *Acta Mater.* **1998**, *46*, 2519.
(26) Kim, H.-M.; Miyaji, F.; Kokubo, T.; Nakamura, T. *J. Biomed. Mater. Res.* **1996**, *32*, 409.
(27) Lianga, F.; Zhoub, L.; Wang, K. *Surf. Coat. Technol.* **2003**, *165*, 133.
(28) Conway, B. E.; Jerkiewicz, G. *Z. Phys. Chem.* **1994**, *183*, 281.
(29) Jerkiewicz, G.; Zolfaghari, A. *J. Electrochem. Soc.* **1996**, *143*, 1240.
(30) Jerkiewicz, G. *Prog. Surf. Sci.* **1998**, *57*, 137.
(31) Qian, S. Y.; Conway, B. E.; Jerkiewicz, G. *Int. J. Hydrogen Energy* **2000**, *25*, 539.
(32) Kubaschewski, O.; Hopkins, B. E. *Oxidation of Metals and Alloys*; Butterworths: London, 1962.
(33) Hauffe, K. *Oxidation of Metals*; Plenum Press: New York, 1965.
(34) Trasatti, S. In *The Electrochemistry of Novel Materials*; Lipkowski, J., Ross, P. N., Eds.; VCH Publishers: New York, 1994; Chapter 5.
(35) Azumi, K.; Nakajima, M.; Okamoto, K.; Seo, M. *Corros. Sci.* **2007**, *49*, 469.
(36) Jerkiewicz, G.; Zhao, B.; Hrapovic, S.; Luan, B. L. *Chem. Mater.* **2008**, *20*, 1877.
(37) Shimogori, K. *Boshoku Gijutsu* **1998**, *30*, 349.
(38) Fukuzuka, T.; Shimogori, K.; Satoh, H.; Tomari, H. *Boshoku Gijutsu* **1979**, *28*, 379.
(39) Ohtsuka, T.; Masuda, M.; Seo, M. *J. Electrochem. Soc.* **1985**, *132*, 787.
(40) Emsley, J. *The Elements*, 3rd ed.; Oxford University Press: Oxford, U.K., 2000.
(41) Conway, B. E. *Ionic Hydration in Chemistry and Biophysics*; Elsevier: Amsterdam, The Netherlands, 1981.

AM900474H